Neuron, Vol. 20, 235–243, February, 1998, Copyright ©1998 by Cell Press

Ephrin-A5 (AL-1/RAGS) Is Essential for Proper Retinal Axon Guidance and Topographic Mapping in the Mammalian Visual System

Jonas Frisén,*‡‖ Paul A. Yates,†‡
Todd McLaughlin,† Glenn C. Friedman,†
Dennis D. M. O'Leary,†§# and Mariano Barbacid*§#
*Department of Molecular Oncology
Bristol-Myers Squibb Pharmaceutical Research Institute
Princeton, New Jersey 08543
†Molecular Neurobiology Laboratory
The Salk Institute
La Jolla, California 92037

Summary

Ephrin-A5 (AL-1/RAGS), a ligand for Eph receptor tyrosine kinases, repels retinal axons in vitro and has a graded expression in the superior colliculus (SC), the major midbrain target of retinal ganglion cells. These properties implicate ephrin-A5 in the formation of topographic maps, a fundamental organizational feature of the nervous system. To test this hypothesis, we generated mice lacking *ephrin-A5*. The majority of *ephrin-A5*$^{-/-}$ mice develop to adulthood, are morphologically intact, and have normal anterior–posterior patterning of the midbrain. However, within the SC, retinal axons establish and maintain dense arborizations at topographically incorrect sites that correlate with locations of low expression of the related ligand *ephrin-A2*. In addition, retinal axons transiently overshoot the SC and extend aberrantly into the inferior colliculus (IC). This defect is consistent with the high level of *ephrin-A5* expression in the IC and the finding that retinal axon growth on membranes from wild-type IC is inhibited relative to that on membranes from *ephrin-A5*$^{-/-}$ IC. These findings show that ephrin-A5 is required for the proper guidance and mapping of retinal axons in the mammalian midbrain.

Introduction

The Eph family of receptors, the largest subgroup of receptor tyrosine kinases (Tuzi and Gullick, 1994; Brambilla and Klein, 1995), bind a family of cell surface proteins known as ephrins (Eph Nomenclature Committee, 1997), which are anchored to the plasma membrane either by a glycosyl phosphatidylinositol (GPI) linkage (ephrins A1–A5) or by a single transmembrane domain (ephrins B1–B3) (Pandey et al., 1995). With few exceptions, GPI-linked ephrins activate the subgroup A of Eph receptors (EphA1–EphA8), whereas the transmembrane ephrins activate the subgroup B of Eph receptors (EphB1–EphB6) (Eph Nomenclature Committee, 1997; Orioli and Klein, 1997).

Ephrins and their receptors are often expressed in complementary and mutually exclusive patterns that demarcate boundaries between different structural regions during development, suggesting a role in patterning of the embryo (Friedman and O'Leary, 1996a; Lumsden and Krumlauf, 1996; Gale et al., 1996). Functional evidence has been recently obtained in *Xenopus* and zebrafish embryos, in which ectopic expression of truncated, dominant negative EphA4 results in improper regionalization of the developing hindbrain and forebrain (Xu et al., 1995, 1996). Additionally, ephrins and their receptors have been implicated in axonal guidance (Tessier-Lavigne, 1995; Tessier-Lavigne and Goodman, 1996). To date, an in vivo loss-of-function analysis for ephrins has not been reported, although mice with targeted deletions of Eph receptors have been studied. Mice lacking EphB2 (Henkemeyer et al., 1996) and EphB3 (Orioli et al., 1996) have defects in the development of forebrain axonal commissures and a high incidence of cleft palate. In addition, targeted deletion of *EphA8* results in abnormal axonal projections that originate in a subset of midbrain neurons that normally express this receptor (Park et al., 1997).

Ephrins may also have a role in the development of topographic axonal projections (Friedman and O'Leary, 1996a; Drescher et al., 1997). The preeminent model for studies on the formation of topographic maps has been the retinotectal projection (retinocollicular projection in mammals), where retinal ganglion cell axons innervate the tectum following a spatial order determined by their respective positions in the retina. Sperry (1963) proposed in his chemoaffinity hypothesis that graded distributions of molecules in the tectum and in the retina confer positional addresses and control the topographic targeting of retinal axons. *ephrin-A2* (Cheng and Flanagan, 1994) and *ephrin-A5* (Drescher et al., 1995; Winslow et al., 1995) are expressed in chicks in an increasing rostral–caudal gradient in the tectum and their preferred receptor, *EphA3*, in an increasing gradient from nasal to temporal retina, consistent with a potential role for ephrin-A2 and ephrin-A5 in providing positional information for developing retinotectal axons (Cheng et al., 1995; Drescher et al., 1995; Monschau et al., 1997). In mice, *ephrin-A2* (Zhang et al., 1996) and *ephrin-A5* (Donoghue et al., 1996; Zhang et al., 1996) are expressed in the embryonic superior colliculus (SC), with *ephrin-A5* transcripts present in a low rostral to high caudal gradient (Donoghue et al., 1996), and ligand binding activity indicates a high temporal to low nasal gradient of EphA receptors (Marcus et al., 1996). In vitro, ephrin-A2 and ephrin-A5 repel retinal axons and cause the collapse of their growth cones (Drescher et al., 1995; Nakamoto et al., 1996; Brennan et al., 1997; Meima et al., 1997; Monschau et al., 1997). Moreover, temporal axons avoid areas of ectopic expression of *ephrin-A2* in the rostral tectum of chickens infected with an *ephrin-A2*–expressing retrovirus (Nakamoto et al., 1996). However, the functional significance of ephrins and the consequence of

‡These authors contributed equally to this work.
§These investigators are co–senior authors.
‖Present address: Department of Cell and Molecular Biology, Medical Nobel Institute, Karolinska Institute, S-171 77 Stockholm, Sweden.
#To whom correspondence should be addressed.

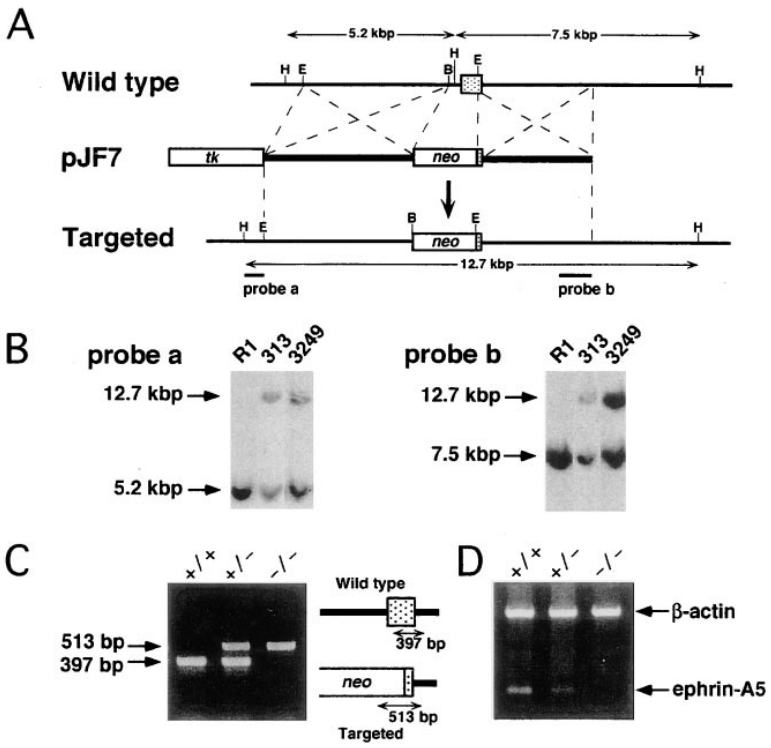

Figure 1. Generation of *ephrin-A5*$^{-/-}$ Mice

(A) Schematic diagram of the strategy used to target the *ephrin-A5* gene. At the top is a partial restriction map of 129/Sv genomic DNA encompassing the targeted exon (stippled box) (H, HindIII; E, EcoRI; B, BamHI). In the center is the targeting vector, *pJF7*, which contains the *PGK-neo* (open box, *neo*) and PGK-thymidine kinase (open box, *tk*) cassettes. At the bottom is a schematic diagram of the predicted targeted allele resulting from homologous recombination between the wild-type allele and the targeting vector. Sequences used for Southern blot analysis of recombinant ES cell clones and probes a and b are indicated by black bars. Probes a and b recognize wild-type HindIII DNA fragments of 5.2 kb and 7.5 kb, respectively. Both probes recognize the same 12.7 kb HindIII DNA fragment in the targeted allele.

(B) Southern blot analysis of the parental ES cells (R1) and the two recombinant clones (P7–313 and P7–3249) used to generate chimeric mice. Probes a and b are those described in (A). The size and migration of the resulting HindIII DNA fragments is indicated.

(C) PCR-aided amplification of DNAs isolated from tails of wild-type (+/+), heterozygous (+/−), and homozygous (−/−) littermates derived from crosses between *ephrin-A5*$^{+/-}$ mice. Migration of DNA fragments derived from wild-type (+) (397 bp) and targeted (−) (513 bp) alleles is indicated by arrowheads. The strategy used to amplify these sequences is also indicated. Primers are indicated by arrows. Boxes are those described in (A).

(D) RT-PCR analysis of *ephrin-A5* and β-actin mRNA expression in brains of newborn *ephrin-A5*$^{+/+}$, *ephrin-A5*$^{+/-}$, and *ephrin-A5*$^{-/-}$ mice is also shown.

the loss of ephrin expression for retinal axon guidance and topographic map formation remains unknown.

Results

Generation of *ephrin-A5*$^{-/-}$ Mice

To test whether ephrin-A5 is required for the proper development of the retinocollicular projection, we have generated gene-targeted mice carrying a null mutation in the gene encoding ephrin-A5 (Figure 1). The majority of these mice reach adulthood, are fertile, and do not display any overt morphological or behavioral defects. However, a subpopulation of newborn *ephrin-A5*$^{-/-}$ mice (17% [17 of 100 born]) display defects in the dorsal midline of the head with various degrees of penetrance (data not shown). The mildest cases display a hematoma or a small aperture in the dorsal midline of the cranium with a discrete protrusion of brain tissue covered by meninges and skin. The more severely affected mice have completely open craniums with cleft nose and palate and absence of brain (anencephaly), pituitary gland, and trigeminal ganglia. All anencephalic mice die immediately after birth. Anaylses of retinal axon guidance and topographic mapping were done in *ephrin-A5*$^{-/-}$ mice that had no obvious morphological defects of the cranium or brain.

To rule out that an undetected defect compromises the midbrain in the *ephrin-A5*$^{-/-}$ mice, which in turn might indirectly affect retinal axon patterning, we carried out a more detailed assessment of the neuroanatomy and gene expression in these mice. Examination of postnatal day 0–1 (P0–P1) brain sections indicated that all of the major brain commissures, including the dorsal midbrain commissures (habenular commissure, the posterior commissure, and the commissures of the superior and inferior colliculi), appear normal in *ephrin-A5*$^{-/-}$ mice. In wild-type mice, *ephrin-A5* is expressed in the colliculi during the development of the retinocollicular projection. *ephrin-A5* has high expression in the inferior colliculus (IC) and a decreasing gradient of expression from caudal to rostral SC in embryonic (Donoghue et al., 1996; Zhang et al., 1996) and neonatal (Figure 2A) mice. In contrast, *ephrin-A2* expression is not evident in the IC in either embryonic (Zhang et al., 1996) or neonatal (Figure 2B) mice but is relatively high throughout much of the SC, with lower levels in rostral and caudal-most SC. The pattern of *ephrin-A2* expression in the SC of P0 *ephrin-A5*$^{-/-}$ mice is indistinguishable from that in wild-type mice (compare Figures 2B and 2C). In addition, the expression of the homeodomain transcription factors *En-1* (Figures 2D and 2E) and *En-2* (data not shown), which regulate the anterior–posterior polarity of the midbrain and of the retinotectal projection (Itasaki and Nakamura, 1992, 1996; Friedman and O'Leary, 1996b), are similar in wild-type and *ephrin-A5*$^{-/-}$ midbrain (compare Figures 2D and 2E). Taken together, these findings indicate that the anatomical integrity and the anterior–posterior polarity of the midbrain is unaffected in the *ephrin-A5*$^{-/-}$ mice used for the analyses of retinal axon targeting.

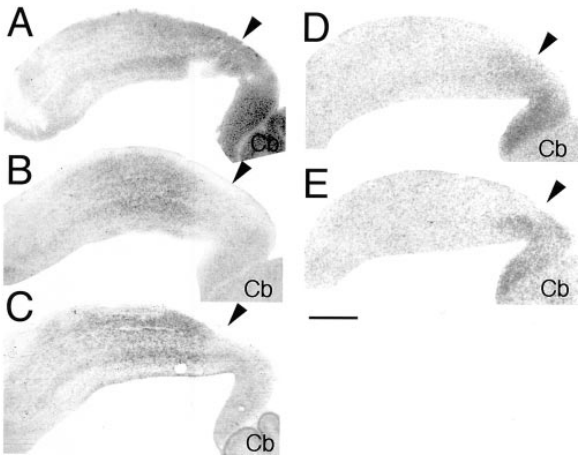

Figure 2. Expression of Midbrain Markers in Wild-Type and *ephrin-A5*$^{-/-}$ Mice

Expression of *ephrin-A5* (A), *ephrin-A2* ([B] and [C]), and *En-1* ([D] and [E]) detected by in situ hybridization with digoxygenin-labeled ([A], [B], and [C]) or ^{35}S-labeled ([D] and [E]) antisense riboprobes on 20 μm sagittal cryosections of P0–P1 wild-type ([A], [B], and [D]) and *ephrin-A5*$^{-/-}$ ([C] and [E]) mouse brain. Arrowheads approximate the border between the superior colliculus (SC) and the inferior colliculus (IC); the SC is rostral to the arrowhead (i.e., to the left), and the IC is caudal to it (i.e., to the right). Cb, cerebellum.

(A) Expression of *ephrin-A5* is highest in caudal IC and decreases in a caudal to rostral gradient through the SC.

(B and C) *ephrin-A2* has high expression through much of the SC, with low or nondetectable expression in caudal-most and rostral SC and in the IC. *ephrin-A2* expression is similar in wild-type and *ephrin-A5*$^{-/-}$ mice.

(D and E) Expression of *En-1* in wild-type mouse midbrain (D) is similar to that in *ephrin-A5*$^{-/-}$ midbrain (E). Sections were exposed to X-ray film for 4 days; images were photographed from the films. No specific signal was detected when sections were hybridized with sense probes (data not shown). Further, *ephrin-A5* expression using antisense digoxygenin riboprobes was not detected in sections from *ephrin-A5*$^{-/-}$ brains (data not shown). Scale bar, 500 μm.

Ephrin-A5 Is Required for Proper Topographic Mapping of Retinal Axons in the Superior Colliculus

Retinal axons first reach the contralateral SC on embryonic day 14 (E14). However, topographic order in the retinocollicular projection emerges later, during the first postnatal week, through remodeling of an initially diffuse projection (Simon and O'Leary, 1992a, 1992b; Yates and O'Leary, unpublished data). Therefore, we assessed the requirement of ephrin-A5 for topographic mapping in P11–P15 mice, many days after order is normally established, using anterograde and retrograde tracing of retinal axons. Anterograde analysis was done by making small focal injections of DiI in temporal retina, which expresses the highest levels of EphA receptors (Marcus et al., 1996), and retrograde analysis with focal injections of DiI in caudal SC, which expresses the highest levels of *ephrin-A5* (Donoghue et al., 1996). These complementary approaches reveal the distribution in the SC of axons arising from a specific site in the retina and the distribution of retinal ganglion cells that send axons to a specific site in the SC. Analyses were done on the SC and retina contralateral to the injections.

In wild-type mice (n = 7), labeled temporal retinal axons project exclusively to the topographically appropriate site in rostral SC where they densely arborize in a focused termination zone (TZ) (Figure 3A). In *ephrin-A5*$^{-/-}$ mice (n = 16), labeled temporal axons arborize at the topographically appropriate TZ in rostral SC; however, in half of these cases we also observe topographically aberrant projections (Figures 3B and 3C). In each of these cases (n = 8), a proportion of the labeled temporal axons continue caudally across the SC and arborize in a dense, well-focused ectopic TZ in the caudal-most SC near its border with the IC. In addition, aberrant arborizations are observed elsewhere in the SC, most typically in rostral SC (Figures 3B and 3C). Aberrant arborizations are infrequently observed in mid-caudal SC, and when present they are much less dense than those found at other sites. Thus, temporal retinal axons map to both appropriate and inappropriate sites in the SC of *ephrin-A5*$^{-/-}$ mice. The pattern of aberrant arborizations in the *ephrin-A5*$^{-/-}$ SC has never been observed in wild-type SC at any developmental stage (Simon and O'Leary, 1992a, 1992b; Yates and O'Leary, unpublished data). Therefore, the aberrant topographic map cannot be due to arresting a normal developmental process at an immature stage.

Retrograde labeling from the SC confirms the topographic aberrancies shown by anterograde labeling. In both wild-type (n = 6) and *ephrin-A5*$^{-/-}$ mice (n = 6), DiI injections in the caudal-most SC retrogradely label a focused cluster of ganglion cells in the topographically correct location in peripheral nasal retina (Figures 3D and 3E). However, in every *ephrin-A5*$^{-/-}$ case, a sizable number of labeled ganglion cells is also scattered across the retina (Figure 3E). Counts of labeled ganglion cells in the topographically inappropriate temporal retina reveal a significant 20-fold increase in *ephrin-A5*$^{-/-}$ mice compared to wild-type mice (161 ± 32 [SEM] versus 8 ± 2 [SEM] per retina; $p < 0.001$). Therefore, all *ephrin-A5*$^{-/-}$ mice likely have an aberrant topographic map, even though we only observe aberrant retinal projections in half of the anterogradely labeled cases. In contrast to the aberrant distribution of ganglion cells labeled from the caudal-most SC, the distribution of ganglion cells retrogradely labeled by DiI injected into mid-caudal SC is similar in wild-type (n = 3) and *ephrin-A5*$^{-/-}$ mice (n = 2). Mid-caudal SC injections label a focused cluster of ganglion cells at the topographically appropriate location in nasal retina but very few cells elsewhere in the retina (Figures 3F and 3G). This finding is consistent with the paucity of aberrant arborizations in mid-caudal SC in the anterograde labeling cases (Figures 3B and 3C). Taken together, these results indicate that ephrin-A5 is required for the development of the normal topographic organization of the retinocollicular projection.

Early Retinal Axon Guidance Defects in *ephrin-A5*$^{-/-}$ Mice

The high level of *ephrin-A5* expression in the IC relative to the SC, along with in vitro data showing that ephrin-A5 repels or collapses retinal axon growth cones (Drescher et al., 1995; Meima et al., 1997; Monschau et al., 1997), suggests that it may have a role in restricting retinal axons to their target, the SC, preventing them

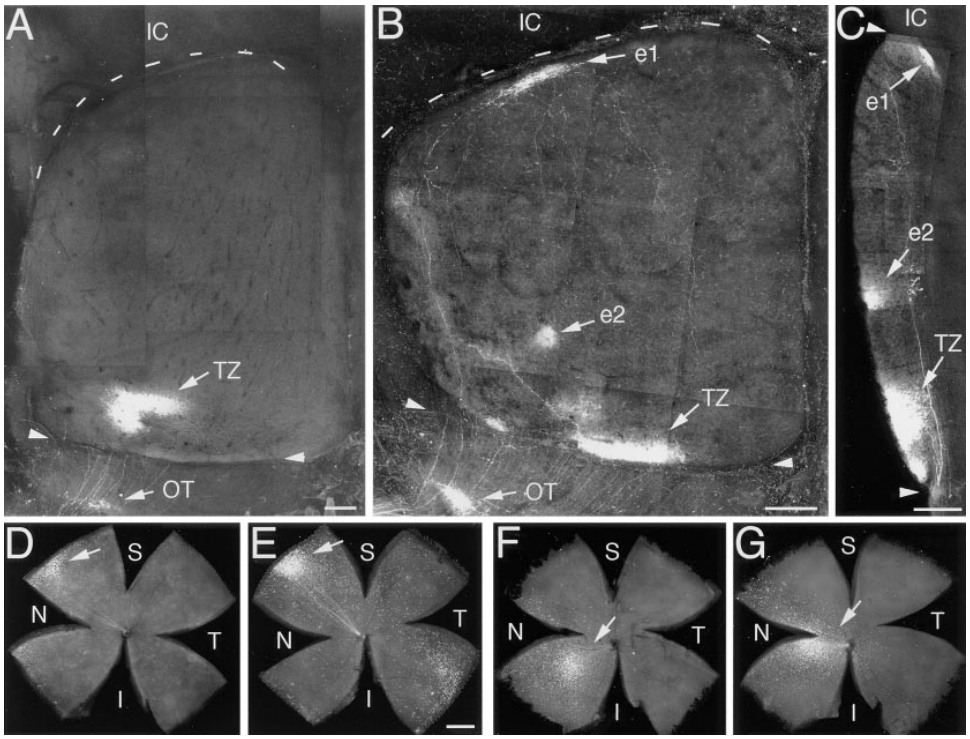

Figure 3. Aberrant Topographic Mapping of Retinal Axons in the Superior Colliculus (SC) of *ephrin-A5*$^{-/-}$ Mice

Anterograde ([A] through [C]) and retrograde ([D] through [G]) DiI labeling of retinal ganglion cell axons in wild-type ([A], [D], and [F]) and *ephrin-A5*$^{-/-}$ ([B], [C], [E], and [G]) mice.

(A–C) Anterograde DiI labeling of retinal axons from temporal retina at P15 ([A] and [C]) and P11 (B). Rostral SC is to the bottom and arrowheads mark its border.

(A and B) Dorsal views of whole mounts of the SC and inferior colliculus (IC); midline is to the right and the dashed line indicates the caudal SC border.

(A) In wild-type mice, the labeled temporal retinal axons end and arborize in a densely labeled termination zone (TZ) in rostral SC. The retinal projection to an optic tract nucleus is also evident (OT).

(B) In *ephrin-A5*$^{-/-}$ mice, labeled temporal retinal axons also end and arborize in a densely labeled TZ at the topographically appropriate site in rostral SC, but in addition labeled axons project to and arborize at topographically inappropriate sites located in caudal-most SC (e1) and in rostral SC (e2).

(C) A 100 μm sagittal section through the SC of another *ephrin-A5*$^{-/-}$ case also showing a normal TZ in addition to topographically aberrant arborizations in rostral (e2) and caudal-most (e1) SC; the border between the SC and IC is marked with an arrowhead.

(D–G) Retrograde labeling in the retina at P13 following DiI injections at P12 into the SC.

(D and E) Injections into caudal-most SC retrogradely labeled a dense cluster of ganglion cells in peripheral nasal retina (arrows) in both wild-type (D) and *ephrin-A5*$^{-/-}$ (E) mice. In wild-type retina, few labeled cells are present outside of the dense cluster. However, in the *ephrin-A5*$^{-/-}$ retina, a substantial number of labeled cells are present across much of the retina.

(F and G) Injections into mid-caudal SC retrogradely labeled a dense cluster of ganglion cells in mid-nasal retina (arrows) in both wild-type (F) and *ephrin-A5*$^{-/-}$ (G) mice. Only a few scattered cells are seen in temporal retina. I, inferior; S, superior; N, nasal; T, temporal. Scale bars: (A–C) 200 μm, (E) 500 μm. Scale bar in (E) is the same for (D) through (G).

from overshooting into the IC. To address this hypothesis, we examined the targeting of temporal retinal axons in P1–P2 mice using anterograde and retrograde axon labeling. In wild-type mice ($n = 9$), temporal retinal axons extend across the entire rostral–caudal axis of the contralateral SC, and only a small number continues caudally into the IC (Figure 4A). In every *ephrin-A5*$^{-/-}$ case ($n = 13$), a substantially greater number of labeled axons overshoot into the IC (Figure 4B). In both wild-type and *ephrin-A5*$^{-/-}$ mice, the overshooting axons are fasciculated, remain at the surface, do not arborize, and continue into caudal-most IC (Figures 4C and 4D). However, the fascicles of overshooting axons are substantially thicker in the *ephrin-A5*$^{-/-}$ mice than in wild-type littermates. Examination of counterstained sections does not reveal architectural differences between wild-type and *ephrin-A5*$^{-/-}$ mice at the border of the SC and IC (data not shown). DiI injections into caudal IC retrogradely label significantly fewer ganglion cells in the contralateral retina of wild-type mice (Figure 4E; $n = 9$; 176 ± 56 [SEM] per retina) compared to the *ephrin-A5*$^{-/-}$ mice (Figure 4F; $n = 13$; 632 ± 112 [SEM]; $p < 0.005$), confirming the anterograde findings. In wild-type mice, the distribution of labeled ganglion cells is biased, with a significantly greater number in nasal retina (138 ± 45 [SEM]) compared to temporal retina (38 ± 11 [SEM]; $p < 0.05$). In contrast, in the *ephrin-A5*$^{-/-}$ mice, the labeled ganglion cells are uniformly distributed across the retina, with no significant difference in the number labeled in nasal retina compared to temporal retina (336 ± 58 [SEM] versus 296 ± 56 [SEM]; $p = 0.62$). These findings demonstrate that in the absence of ephrin-A5,

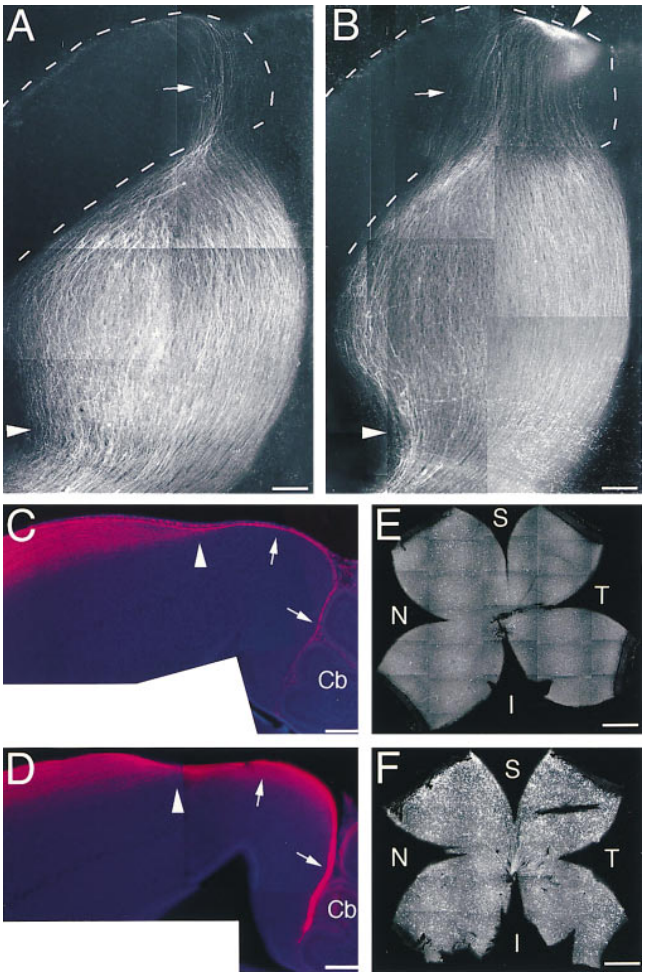

Figure 4. Aberrant Growth of Retinal Axons into the Inferior Colliculus (IC) in *ephrin-A5*$^{-/-}$ Mice

(A and B) Dorsal views of whole mounts of the superior colliculus (SC) and IC from P2 wild-type (A) and *ephrin-A5*$^{-/-}$ (B) mice showing DiI-labeled axons from temporal retina. Arrowheads mark the rostral border of the SC with the optic tract. Dashed lines outline the IC. In contrast to the small number of labeled retinal axons that extend into the IC in wild-type mice (arrow in [A]), a substantial number extend aberrantly into the IC in *ephrin-A5*$^{-/-}$ mice (arrow in [B]). The bright labeling (arrowhead at the top of [B]) is not a termination zone but is an optical effect of retinal axons following the curved surface of the IC.

(C and D) Sagittal sections (100 μm) through the caudal SC and the IC of P2 wild-type (C) and *ephrin-A5*$^{-/-}$ (D) mice shows that labeled retinal axons that extend into the IC are fasciculated and remain at the surface. The panels are overlays of the DiI-labeled axons and counterstaining with bisbenzimide. The arrowhead approximates the border between the SC and the IC.

(E and F) Retinal wholemounts from P2 wild-type (E) and *ephrin-A5*$^{-/-}$ (F) mice show the distribution of ganglion cells retrogradely labeled with DiI injected into caudal IC at P1. I, inferior; S, superior; N, nasal; T, temporal. The number of retrogradely labeled cells is dramatically increased in number and distribution in the *ephrin-A5*$^{-/-}$ mice compared to wild-type. Scale bars: (A, B, C, and D) 200 μm, (E and F) 500 μm.

retinal axons are not restricted to their proper midbrain target, the SC, and overshoot it aberrantly into the IC.

The aberrant retinal projection to the IC is not maintained. Anterograde DiI labeling from temporal retina in P11–P15 mice does not reveal any axons extending into the IC in wild-type or *ephrin-A5*$^{-/-}$ mice (Figures 3A–3C). In addition, in P13 mice, DiI injections into the IC label few ganglion cells in either wild-type ($n = 3$; 9 ± 2 [SEM]) or *ephrin-A5*$^{-/-}$ retinas ($n = 7$; 24 ± 5 [SEM]). Thus, even in the absence of ephrin-A5, the IC lacks the ability to support retinal input.

The aberrant overshooting of retinal axons into the IC of *ephrin-A5*$^{-/-}$ mice, together with the high level of *ephrin-A5* expression in the IC in wild-type mice, suggests that ephrin-A5 may act in part to restrict retinal axons to the SC through growth cone repulsion or inhibition. To address this issue, we used an in vitro membrane substrate assay (Walter et al., 1987) previously used to demonstrate retinal axon responses to membrane-associated molecules in the SC (Godement and Bonhoeffer, 1989; Simon and O'Leary, 1992b; Roskies and O'Leary, 1994). Retinal explants from E14–E16 wild-type mice were grown on homogenous carpets of membranes prepared from the SC or IC of P0–P2 wild-type and *ephrin-A5*$^{-/-}$ mice; neurite outgrowth was scored on a 0–4 scale (see Experimental Procedures). There is no significant difference in retinal neurite outgrowth between SC membranes from wild-type (Figure 5A; $n = 14$; 1.8 ± 0.3 [SEM]) compared to *ephrin-A5*$^{-/-}$ (Figure 5B; $n = 7$; 2.2 ± 0.5 [SEM]; $p > 0.4$) mice, presumably due to the presence of ephrin-A2 in the SC. In contrast, retinal neurite outgrowth is significantly less on IC membranes from wild-type (Figure 5C; $n = 12$; 1.0 ± 0.4 [SEM]) compared to *ephrin-A5*$^{-/-}$ (Figure 5D; $n = 8$; 2.4 ± 0.4 [SEM]; $p < 0.02$) mice. These findings suggest that ephrin-A5 in the IC inhibits retinal axon growth.

Discussion

Our analyses of morphologically normal *ephrin-A5*$^{-/-}$ mice have revealed substantial aberrancies in the topographic organization of the retinocollicular projection and, at earlier stages, defects in retinal axon guidance within the midbrain. Two sets of findings render it unlikely that these effects on retinal axon targeting are due to a defect in anterior–posterior (i.e., rostral–caudal) patterning of the midbrain other than the lack of ephrin-A5. First, the dorsal midbrain is anatomically intact, including midline structures such as axonal commissures, the positioning and size of which would seemingly be influenced by both anterior–posterior and dorsal–ventral

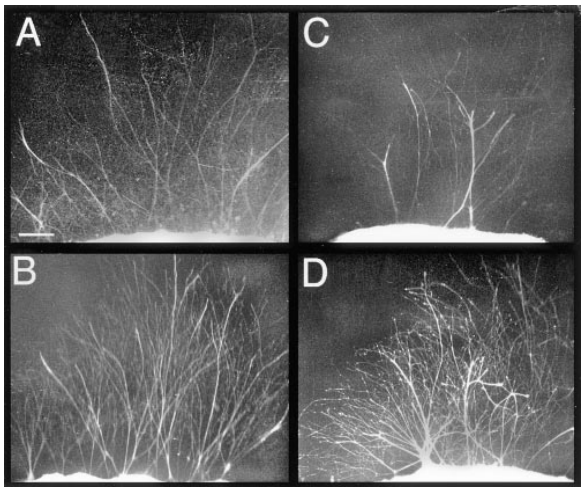

Figure 5. Ephrin-A5 Inhibits Retinal Axon Growth In Vitro

Retinal explants from E14–E16 wild-type mice grown on homogeneous carpets of membranes from the caudal half of the superior colliculus (SC) from P0–P2 wild-type (A) or *ephrin-A5*$^{-/-}$ (B) mice or from the inferior colliculus (IC) of P0–P2 wild-type (C) or *ephrin-A5*$^{-/-}$ (D) mice. Retinal neurites were labeled with the vital dye carboxyfluoroscein. There was no significant difference in retinal neurite outgrowth between membranes from wild-type (A) or *ephrin-A5*$^{-/-}$ (B) SC. In contrast, retinal axon outgrowth was significantly poorer on membranes from wild-type IC (C) compared to membranes from *ephrin-A5*$^{-/-}$ IC (D). The explants shown have neurite outgrowth that approximates the mean score for each type of membrane substrate (see Experimental Procedures). Scale bar, 200 μm.

patterning cues. Further, the anterior–posterior patterning of the midbrain appears normal in *ephrin-A5*$^{-/-}$ mice, as defined by the expression patterns of *ephrin-A2* and the *engrailed* genes *En-1* and *En-2*, which confer anterior–posterior polarity to the midbrain (Itasaki and Nakamura, 1992, 1996; Friedman and O'Leary, 1996b) and regulate the expression of *ephrin-A5* and *ephrin-A2* (Logan et al., 1996; Shigetani et al., 1997). These findings indicate that the defects in retinal axon patterning in the midbrain of *ephrin-A5*$^{-/-}$ mice are the direct consequence of the lack of ephrin-A5 and its normal influence on retinal axon targeting.

Ephrin-A2 and ephrin-A5 have been hypothesized to guide retinal axons to their correct topographic locations in the optic tectum through growth cone repulsion or inhibition, based on their smooth, increasing rostral to caudal graded distributions in the chick optic tectum and their ability to differentially repel temporal and nasal retinal axons in vitro (Nakamoto et al., 1996; Monschau et al., 1997). Such a gradient model would predict several possible organizations for the retinal projection in the absence of ephrin-A5, including (1) a topographically appropriate map if ephrin-A2 fully compensated for the loss of ephrin-A5, (2) a topographic map that would shift caudally in an orderly manner if ephrin-A2 partially compensated for the loss of ephrin-A5, and (3) a projection that would have no topographic order along the rostral–caudal axis if ephrin-A2 did not compensate at all for the loss of ephrin-A5. Our findings do not fit with these predictions. The first prediction is readily discounted, since the topographic organization of the retinocollicular projection is clearly aberrant in the *ephrin-A5*$^{-/-}$ mice. The second prediction is inconsistent with our finding that ganglion cells at the same retinal location aberrantly project to multiple sites along the rostral–caudal axis of the SC, rather than to a single location that is shifted caudally in the SC. Finally, the third prediction is inconsistent with our finding of topographically appropriate arborizations of temporal retinal axons in rostral SC of *ephrin-A5*$^{-/-}$ mice.

Although our findings are inconsistent with this gradient model, the distribution of the aberrant projections that we observe in the *ephrin-A5*$^{-/-}$ mice do appear to relate to the expression pattern of *ephrin-A5* relative to *ephrin-A2*. During normal development of the rodent retinocollicular projection, retinal axons grow well past their topographically correct locations along the rostral–caudal SC axis. Topographic order is established through a bias in the branching of retinal axons at their topographically correct locations along the rostral–caudal axis, followed by a remodeling phase during which appropriately positioned branches form stable arbors and inappropriate segments of retinal axons are eliminated (Simon and O'Leary, 1992a, 1992b; Yates and O'Leary, unpublished data). During normal development, a prominent function of ephrin-A5 and ephrin-A2 may be to prevent retinal axon branching and arborization at topographically inappropriate locations. This proposal is supported by the in vitro demonstration that temporal retinal axons show a strong preference to branch on membrane preparations from topographically appropriate rostral SC, which contains low levels of ephrin-A2 and ephrin-A5, and are inhibited from branching on membranes from topographically inappropriate caudal SC, which contain high levels of ephrin-A2 and ephrin-A5. Removal of GPI-anchored molecules such as ephrin-A2 and ephrin-A5 from the caudal membranes eliminates the branching specificity of temporal axons for rostral membranes (Roskies and O'Leary, 1994).

In *ephrin-A5*$^{-/-}$ mice, temporal axons aberrantly arborize in caudal-most SC as well as at topographically correct and incorrect locations in rostral SC. Aberrant arborizations are infrequently found in mid-SC, where *ephrin-A2* is most highly expressed. Thus, in *ephrin-A5*$^{-/-}$ mice, the aberrant arbors are most frequently found in parts of the SC where *ephrin-A5* would normally be expressed and *ephrin-A2* is expressed at low levels (Figure 6). We suggest that in *ephrin-A5*$^{-/-}$ mice, retinal axons branch and arborize at reproducible but topographically inappropriate locations in the SC because of the lack of the repellent activity of ephrin-A5, and because the low level of ephrin-A2 repellent activity at these locations is insufficient to compensate for the lack of ephrin-A5. These in vivo findings in *ephrin-A5*$^{-/-}$ mice are consistent with in vitro findings that GPI-linked repellent molecules regulate topographic specificity in retinal axon branching and arborization by inhibiting their formation and stabilization at inappropriate locations (Roskies and O'Leary, 1994). The distribution of the aberrant arbors at multiple, widely separated sites along the rostral–caudal SC axis in the *ephrin-A5*$^{-/-}$ mice suggests that ephrin-A2 by itself does not form a smooth rostral to caudal gradient of repellent activity across the entire SC. However, in the normal SC, ephrin-A2 and ephrin-A5 together may form a smooth gradient of repellent activity across the SC. These inferences drawn from the topographic mapping of retinal axons in wild-type

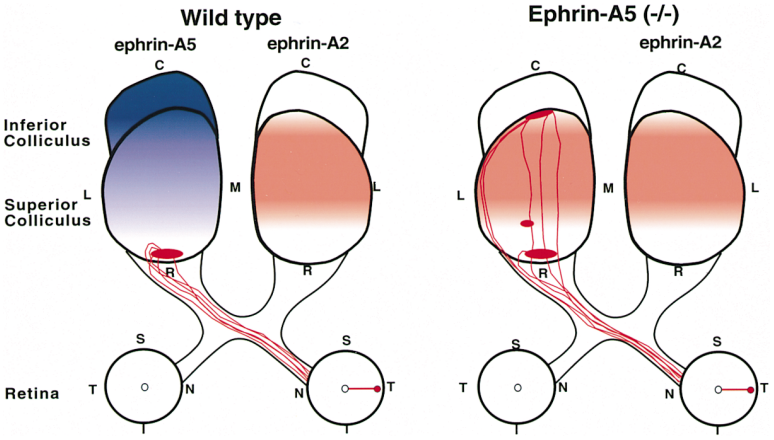

Figure 6. Relationship of Topographically Aberrant Retinal Projections in *ephrin-A5*$^{-/-}$ Mice to Expression Domains of *ephrin-A5* and *ephrin-A2*

In wild-type mice, focal injections of DiI into temporal retina label a dense termination zone in topographically appropriate rostral superior colliculus (SC). The distinct expression patterns of *ephrin-A5* and *ephrin-A2* may together form a smooth repellent gradient across the colliculus and work in concert to help establish the normal topographic map. In *ephrin-A5*$^{-/-}$ mice, injections of DiI into temporal retina label termination zones at both topographically appropriate and inappropriate locations in the SC. The pattern of ectopic arbors relates to the expression pattern of *ephrin-A2*. Ectopic arbors occur most frequently in caudal-most and rostral SC, where there is low *ephrin-A2* expression, but are found rarely in mid-SC, where there is high *ephrin-A2* expression. This reproducible distribution suggests that in the absence of ephrin-A5, abberancies are present where the levels of repellent activity due to ephrin-A2 are too low to prevent the stabilization of ectopic temporal arbors. C, caudal; I, inferior; L, lateral; M, medial; N, nasal; R, rostral; S, superior; T, temporal.

compared to *ephrin-A5*$^{-/-}$ mice are consistent with the differences in the distributions of *ephrin-A5* and *ephrin-A2* transcripts in the SC (present study; Donoghue et al., 1996; Zhang et al., 1996) and the high caudal to low rostral graded binding of receptor-affinity probes, which reveals the overall distribution of ephrin-A ligands in the SC (Zhang et al., 1996). We propose that this gradient of repellent activity mediated by ephrin-A ligands helps control topographic specificity in retinal axon branching and arborization rather than topographic specificity in initial growth cone targeting.

In *ephrin-A5*$^{-/-}$ mice, we also observe a substantial increase in the number of retinal axons that initially overshoot the SC and extend aberrantly into the IC. This suggests that ephrin-A5 helps restrict retinal axons to the SC, their principal midbrain target, and prevents them from continuing their caudal extension into the IC, a nonretinal target. In zebrafish, *L4*, the homolog of *ephrin-A5*, is not expressed in the optic tectum but is highly expressed in a band of tissue immediately caudal to it and has been suggested to form a repellent barrier that restricts retinal axons to the tectum (Brennan et al., 1997). Although the expression of *ephrin-A5* does not form a distinct boundary between the SC and IC in mice, since it is expressed in a graded manner that extends through the IC and continues across the SC, retinal axons do appear to respond to it as if it is a repellent barrier. In vitro data indicates that, as a population, temporal retinal axons elongating on smooth gradients of membranes from caudal tectum, which contain ephrin-A5, are stopped as a function of the steepness of the gradient (Baier and Bonhoeffer, 1992). In addition, our in vitro findings show that neurite outgrowth from wild-type retina is increased on membrane carpets prepared from the IC of *ephrin-A5*$^{-/-}$ mice compared to wild-type mice, which suggests that the level of ephrin-A5 present in the IC inhibits the growth of retinal axons. Together, these findings suggest that in wild-type mice, retinal axons stop in caudal SC because they have reached a point along the ephrin-A5 gradient that halts their growth. This interpretation is further supported by our finding that in wild-type mice, the small number of retinal axons that overshoot into the IC mainly originate from regions of retina that express low levels of EphA receptors, whereas in *ephrin-A5*$^{-/-}$ mice, the substantial increase in the number of overshooting axons appears to be independent of the level of expression of EphA receptors. These results taken together indicate that ephrin-A5 helps to restrict retinal axons to the SC and also controls the topographic mapping of retinal axons within the SC.

Experimental Procedures

Generation of *ephrin-A5*$^{-/-}$ Mice

The 5′ arm of the targeting plasmid was generated by subcloning a 4.5 kb EcoRI–BamHI genomic 129/Sv DNA fragment located upstream of a single *ephrin-A5* exon present in our genomic clones (amino acid residues 42–140) (Winslow et al., 1995) into the EcoRI and BamHI sites of the *pPNT* vector (Tybulewicz et al., 1991). The resulting intermediate plasmid was then used to insert the 3′ arm, a 3.5 kb EcoRI–HindIII DNA fragment containing the last 30 nucleotides of the *ephrin-A5* exon and ~3.5 kb of 3′ intronic sequences (the HindIII site was derived from the phage polylinker) (Figure 1A). The resulting targeting plasmid, pJF7, lacks the 5′ acceptor splicing site of the *ephrin-A5* exon as well as the sequences encoding amino acid residues 42–129, which were replaced by the *PGK-neo* cassette of *pPNT* (Figure 1A). ES cells (R1 clone) were electroporated with pJF7 DNA as previously described (Joyner, 1993). The resulting G418R/GanR clones were submitted to Southern blot analysis, using as probes a 0.4 kb HindIII–EcoRI fragment (probe a) and a 1 kb KpnI–HindIII fragment (probe b) derived from genomic 129/Sv DNA sequences (Figures 1A and 1B). Chimeras derived from two independent clones (P7–313 and P7–3249) transmitted the targeted allele when bred to wild-type C57Bl/6 mice. *ephrin-A5*$^{-/-}$ mice generated from the two different ES clones displayed the same phenotype. Genotyping was performed by PCR using primers 1 (TCCAGCTGTG CAGTTCTCCAAAACA) and 2 (ATTCCAGAGGGGTGACTACCACATT) for amplification of wild-type sequences (397 bp) and primers 1 and 3 (AGCCCAGAAAGCGAAGGAGCAAAGC) for amplification of sequences derived from the targeted allele (513 bp) (Figure 1C).

In Situ Hybridization

In situ hybridization for *ephrin-A5* and *ephrin-A2* was done with digoxygenin-labeled antisense riboprobes on 20 μm thick cryostat sections from fresh-frozen brain tissue as described by Friedman and O'Leary (1996b). The *ephrin-A5* probe corresponded to nucleotides 464–713 (Winslow et al., 1995), and the *ephrin-A2* probe (a gift from Linda Erkman) corresponded to nucleotides 546–1095 (Cheng and Flanagan, 1994). In situ detection of *En-1* and *En-2* was done on 20 μm fresh-frozen sections according to Goulding et al. (1994),

using ^{35}S-labeled antisense riboprobes corresponding to the sequences described by Davis and Joyner (1988).

Anterograde and Retrograde Axonal Labeling

Anterograde and retrograde labeling was done as previously described (Simon and O'Leary, 1992a; Simon et al., 1994). Anterogradely labeled axons in the midbrain contralateral to the injected eye were examined in whole mounts with rhodamine optics on a standard fluorescence microscope or with a BioRad 1000 confocal microscope. Montages were constructed using NIH image and Adobe Photoshop software. The whole mounts were later sectioned sagittally at 100–200 μm on a vibratome, counterstained with bisbenzimide, mounted serially on glass slides, and reexamined as above. For retrograde labeling, DiI was focally injected into the SC or IC. The injected SC or IC and the contralateral retina were prepared as whole mounts and examined as above. Counts of labeled ganglion cells were done blind to genotype on high magnification montages constructed with images collected on the confocal microscope. Statistical significance of the data was determined using Student's unpaired t test.

In Vitro Membrane Carpet Assay

The membrane carpet assay was used as modified by Roskies and O'Leary (Walter et al., 1987; Godement and Bonhoeffer, 1989; Roskies and O'Leary, 1994). Membranes were prepared from the IC or the caudal half of the SC from P0–P2 wild-type (ICR, Harlan Sprague-Dawley) and *ephrin-A5*$^{-/-}$ mice. Retinas were dissected from E14–E16 wild-type mice (ICR) and placed ganglion cell–side down on homogeneous membrane carpets and cultured for 48 hr. Neurite outgrowth was labeled with carboxyfluorescein diacetate and succinimidyl ester (a fluorescent vital dye; Molecular Probes) and photographed under FITC illumination on an upright fluorescence microscope. Observers, blind to the source of membranes, scored outgrowth for each explant on a graded 0–4 scale, in which 0 was no or very sparse outgrowth from a living explant and 4 was very robust growth. Statistical significance of the data was determined using Student's unpaired t test.

Acknowledgments

We thank Soochul Park for helpful discussions, the members of the Transgenic Unit for their help with blastocyst injections, Linda K. Long for genotyping, Douglass Borngasser for help with figure preparation, and Fred Gage for generous access to his confocal microscope. J. F. was supported by the Swedish Medical Research Council. This work was supported in part by NEI grant EY 07025 (D. D. M. O'L.).

Received July 21, 1997; revised January 12, 1998.

References

Baier, H., and Bonhoeffer, F. (1992). Axon guidance by gradients of a target-derived component. Science *255*, 472–475.

Brambilla, R., and Klein, R. (1995). Telling axons where to grow: a role for Eph receptor tyrosine kinases in guidance. Mol. Cell. Neurosci. *6*, 487–495.

Brennan, C., Monschau, B., Lindberg, R., Guthrie, B., Drescher, U., Bonhoeffer, F., and Holder, N. (1997). Two Eph receptor tyrosine kinase ligands control axon growth and may be involved in the creation of the retinotectal map in the zebrafish. Development *124*, 655–664.

Cheng, H.-J., and Flanagan, J.G. (1994). Identification and cloning of Elf-1, a developmentally expressed ligand for the Mek4 and Sek receptor tyrosine kinases. Cell *79*, 157–168.

Cheng, H.-J., Nakamoto, M., Bergemann, A.D., and Flanagan, J.G. (1995). Complementary gradients in expression and binding of Elf-1 and Mek4 in development of the topographic retinotectal projection map. Cell *82*, 371–381.

Davis, C.A., and Joyner, A.L. (1988). Expression patterns of the homeobox-containing genes En-1 and En-2 and the proto-oncogene int-1 diverge during mouse development. Genes Dev. *2*, 1736–1744.

Donoghue, M.J., Merlie, J.P., and Sanes, J.R. (1996). The Eph kinase ligand AL-1 is expressed by rostral muscles and inhibits outgrowth from caudal neurons. Mol. Cell. Neurosci. *8*, 185–198.

Drescher, U., Kremoser, C., Handwerker, C., Löschinger, J., Noda, M., and Bonhoeffer, F. (1995). In vitro guidance of retinal ganglion cell axons by RAGS, a 25 kDa tectal protein related to ligands for Eph receptor tyrosine kinases. Cell *82*, 359–370.

Drescher, U., Bonhoeffer, F., and Müller, B.K. (1997). The Eph family in retinal axon guidance. Curr. Opin. Neurobiol. *7*, 75–80.

Eph Nomenclature Committee. (1997). Unified nomenclature for Eph family receptors and their ligands, the ephrins. Cell *90*, 403–404.

Friedman, G.C., and O'Leary, D.D.M. (1996a). Eph receptor tyrosine kinases and their ligands in neural development. Curr. Opin. Neurobiol. *6*, 127–133.

Friedman, G.C., and O'Leary, D.D.M. (1996b). Retroviral misexpression of engrailed genes in the chick optic tectum perturbs the topographic targeting of retinal axons. J. Neurosci. *17*, 5498–5509.

Gale, N.W., Holland, S.J., Valenzuela, D.M., Flenniken, A., Pan, L., Ryan, T.E., Henkemeyer, M., Strebhardt, K., Hirai, H., Wilkinson, D.G., et al. (1996). Eph receptors and ligands comprise two major specificity subclasses and are reciprocally compartmentalized during embryogenesis. Neuron *17*, 9–19.

Godement, P., and Bonhoeffer, F. (1989). Cross-species recognition of tectal cues by retinal fibers in vitro. Development *106*, 313–320.

Goulding, M., Lumsden, A., and Paquette, A. (1994). Regulation of Pax-3 expression in the dermomyotome and its role in muscle development. Development *120*, 957–971.

Henkemeyer, M., Orioli, D., Henderson, J.T., Saxton, T.M., Roder, J., Pawson, T., and Klein, R. (1996). Nuk controls pathfinding of commissural axons in the mammalian central nervous system. Cell *86*, 35–46.

Itasaki, N., and Nakamura, H. (1992). Rostrocaudal polarity of the tectum in birds: correlation of *en* gradient and topographic order in retinotectal projection. Neuron *8*, 787–798.

Itasaki, N., and Nakamura, H. (1996). A role for gradient *en* expression in positional specification on the optic tectum. Neuron *16*, 55–62.

Joyner, A.L. (1993). Gene Targeting. A Practical Approach. In The Practical Approach Series, D. Rickwood and B.D. Hames, eds. (Oxford: Oxford University Press).

Logan, C., Wizenmann, A., Drescher, U., Monschau, B., Bonhoeffer, F., and Lumsden, A. (1996). Rostral optic tectum acquires caudal characteristics following ectopic *engrailed* expression. Curr. Biol. *6*, 1006–1014.

Lumsden, A., and Krumlauf, R. (1996). Patterning the vertebrate neuraxis. Science *274*, 1109–1115.

Marcus, R.C., Gale, N.W., Morrison, M.E., Mason, C.A., and Yancopoulos, G.D. (1996). Eph family receptors and their ligands distribute in opposing gradients in the developing mouse retina. Dev. Biol. *180*, 786–789.

Meima, L., Kljavin, I.J., Moran, P., Shih, A., Winslow, J.W., and Caras, I.W. (1997). AL-1-induced growth cone collapse of rat cortical neurons is correlated with REK7 expression and rearrangement of the actin cytoskeleton. Eur. J. Neurosci. *9*, 177–188.

Monschau, B., Kremoser, C., Ohta, K., Tanaka, H., Kaneko, T., Yamada, T., Handwerker, C., Hornberger, M., Löschinger, J., Pasquale, E.B., et al. (1997). Shared and unique functions of RAGS and ELF-1 in guiding retinal axons. EMBO J. *16*, 1258–1267.

Nakamoto, M., Cheng, H.-J., Friedman, G.C., McLaughlin, T., Hansen, M.J., Yoon, C.H., O'Leary, D.M.M., and Flanagan, J.G. (1996). Topographically specific effects of Elf-1 on retinal axon guidance in vitro and retinal mapping in vivo. Cell *86*, 755–766.

Orioli, D., and Klein, R. (1997). The Eph receptor family: axonal guidance by contact repulsion. Trends Genet. *13*, 354–359.

Orioli, D., Henkemeyer, M., Lemke, G., Klein, R., and Pawson, T. (1996). Sek4 and Nuk receptors cooperate in guidance of commissural axons and in palate formation. EMBO J. *15*, 6035–6049.

Pandey, A., Lindberg, R.A., and Dixit, V.M. (1995). Receptor orphans find a family. Curr. Biol. *5*, 986–989.

Park, S., Frisén, J., and Barbacid, M. (1997). Aberrant axonal projections in mice lacking Eek tyrosine protein kinase receptors. EMBO J. *16*, 3106–3114.

Roskies, A.L., and O'Leary, D.D.M. (1994). Control of topographic retinal axon branching by membrane-bound molecules. Science *265*, 799–803.

Shigetani, Y., Funahashi, J.-I., and Nakamura, H. (1997). En-2 regulates the expression of the ligands for Eph-type tyrosine kinases in chick embryonic tectum. Neurosci. Res. *27*, 211–217.

Simon, D.K., and O'Leary, D.D.M. (1992a). Development of topographic order in the mammalian retinocollicular projection. J. Neurosci. *12*, 1212–1232.

Simon, D.K., and O'Leary, D.D.M. (1992b). Responses of retinal axons in vivo and in vitro to molecules encoding position in the embryonic superior colliculus. Neuron *9*, 977–989.

Simon, D.K., Roskies, A.L., and O'Leary, D.D.M. (1994). Plasticity in the development of topographic order in the mammalian retinocollicular projection. Dev. Biol. *162*, 384–393.

Sperry, R.W. (1963). Chemoaffinity in the orderly growth of nerve fiber patterns and connections. Proc. Natl. Acad. Sci. USA *50*, 703–710.

Tessier-Lavigne, M. (1995). Eph receptor tyrosine kinases, axon repulsion, and the development of topographic maps. Cell *82*, 345–348.

Tessier-Lavigne, M., and Goodman, C.S. (1996). The molecular biology of axon guidance. Science *274*, 1123–1133.

Tuzi, N.L., and Gullick, W.J. (1994). Eph, the largest known family of putative growth factor receptors. Br. J. Cancer *69*, 417–421.

Tybulewicz, V.L.J., Crawford, C.E., Jackson, P.K., Bronson, R.T., and Mulligan, R.C. (1991). Neonatal lethality and lymphopenia in mice with a homozygous disruption of the *c-abl* proto-oncogene. Cell *65*, 1153–1163.

Walter, J., Kern-Veits, B., Huf, J., Stolze, B., and Bonhoeffer, F. (1987). Recognition of position-specific properties of tectal cell membranes by retinal axons in vitro. Development *101*, 685–696.

Winslow, J.W., Moran, P., Valverde, J., Shih, A., Yuan, J.Q., Wong, S.C., Tsai, S.P., Goddard, A., Henzel, W.J., Hefti, F., et al. (1995). Cloning of AL-1, a ligand for an eph-related tyrosine kinase receptor involved in axon bundle formation. Neuron *14*, 973–981.

Xu, Q.L., Alldus, G., Holder, N., and Wilkinson, D.G. (1995). Expression of truncated Sek-1 receptor tyrosine kinase disrupts the segmental restriction of gene expression in the *Xenopus* and zebrafish forebrain. Development *121*, 4005–4016.

Xu, Q., Alldus, G., Macdonald, R., Wilkinson, D.G., and Holder, N. (1996). Function of the Eph-related kinase rtk1 in patterning of the zebrafish forebrain. Nature *381*, 319–322.

Zhang, J.H., Cerretti, D.P., Yu, T., Flanagan, J.G., and Zhou, R. (1996). Detection of ligands in regions anatomically connected to neurons expressing the Eph receptor Bsk: potential roles in neuron-target interaction. J. Neurosci. *16*, 7182–7192.